


Tracing the potential of rare earth element content in the Adian Koting area, Indonesia

Rita Juliani^{1*} , Rahmatsyah¹, Togi Tampubolon¹, Silvia Dona Sari¹,
Habibi Azka Nasution¹, Riri Syavira², Asla Tara Roma Ito Hutasuhut¹,
Alwi Husain Baeha¹

¹ Department of Physics, Faculty of Mathematics and Natural Sciences, Medan State University, Medan, Indonesia

² Department of Chemistry, Faculty of Mathematics and Natural Sciences, Gadjah Mada University, Yogyakarta, Indonesia

* Corresponding author's e-mail: julianiunimed@gmail.com

ABSTRACT

Rare earth elements (REE) are substitution elements that form in rock-forming minerals and are considered critical energy elements required by industry as part of the energy transition supply chain. The exploration of REE potential aims to identify prospective areas by examining the megascopic and microscopic characteristics of rocks and their elemental composition as natural resources and for the development of priority commodities. The research was conducted in Adian Koting district, north Tapanuli. Rock samples were collected from outcrop areas. The samples were tested using petrological methods with thin sections and polished sections, and geochemical analysis using x-ray fluorescence (XRF) and inductively coupled plasma mass spectrometry (ICP-MS). The samples were prepared in the form of polished sections, which were analyzed using microscopy methods, and ground to a size of 200 mesh for testing using XRF and ICP-MS. The results obtained from the polished sections revealed that the megascopic characteristics of the rocks are coherent igneous rocks, specifically plutonic granite types, with colors ranging from light gray to white with black specks, brownish-white with brick-red to brown patches and black specks, as well as cream to grayish-white with black specks. The rock has an equigranular, hypidiomorphic-granular, and phaneritic texture. The grain shapes are subhedral with a massive structure, composed of minerals such as quartz, plagioclase, biotite, opaque minerals, and hornblende. Microscopically, the rock contains zircon, monazite, and xenotime as REE-bearing minerals. Monazite appears in prismatic, platy, or elongated crystal forms, sometimes large, coarse, and commonly twinned. Monazite and xenotime occur in association, and their presence as inclusions in biotite or quartz indicates early crystallization. Zircon appears as small, bright-colored inclusions. The REE content in the Adiankoting area, based on XRF analysis, shows the presence of Ce and La elements, with Ce concentrations ranging from 74.3 to 97.5 ppm and La concentrations ranging from 90.2 to 141.0 ppm. The ICP-MS test results show the presence of REEs with a dominance of REE elements at concentrations of Sc (3.5–5.5%), La (4.1–5.6%), Y (4–6.1%), Ce (3.5–4.8%), Gd (3.9–5.8%), Tm (5.4–5.6%), Eu (3.1–5.1%). REE and the minimum element include Dy (1.9–3.6%), Yb (0.8–3.5%) and Er (0.473–84.4%). The presence of REE elements indicates that the Adian Koting area has the potential to be a natural resource for industrial technology materials.

Keywords: rare earth element, microscopic, macroscopic, Adian Koting.

INTRODUCTION

Rare earth elements (REE) are substitution elements that form in rock-forming minerals and are classified as critical energy elements, alongside chromium, manganese, and zinc, which are essential for the industry as part of the energy

transition supply chain. REE concentrations are higher than those of industrial and precious metals. The advancement of research in geological resources, exploration, mining, and mineral processing represents an idea and an alternative solution for the sustainable management of mineral resources, particularly REEs. This serves as a

bridge for upstream exploration activities to connect with downstream industrial operations and to develop exploration technologies that can be utilized according to the characteristics of the available resources. REE are used in various high-tech applications across industries such as electrical and electronics, automotive, renewable energy, medical, and defense. The demand for REEs in the global market is increasing day by day due to the needs of various sectors (Dushyantha, 2020).

REE potential is found in both primary and secondary deposits. Primary deposits are formed through magmatic, hydrothermal, and metamorphic processes. These primary deposits are associated with alkaline igneous and carbonatite rocks, including extensional tectonic environments. Secondary deposits are formed as a result of erosion and weathering, including placer, laterite, and bauxite deposits. Rare earth element deposits occur in seven types of deposits: Iron-REE deposits, carbonatite deposits, laterite deposits, placer deposits, REE in peralkaline rocks, REE in veins, and marine sediment REE (Castor and Hedrick, 2016). Sumatra has deposits of 23 million tons with laterite-type deposits rich in iron and aluminum oxides, formed as a result of intense weathering in humid tropical climates, and 5 million tons of tailings-type REE deposits (Idris, 2023). The Adiankoting area is a humid tropical region covering an area of 50,290 hectares, located at an elevation of 200–1600 meters above sea level, with hilly and valley topography and a temperature of 12–28 °C (Figure 1). Topography, rock type, and weathering influence the presence and concentration of REE. Igneous and metamorphic rock types have REE potential. Weathering of rocks, influenced by topography and climate, affects the release of REE-bearing minerals, forming laterite or alluvial deposits. Areas with

high rainfall, ranging from 1500 to 3000 mm per year, and complex topography tend to experience intense weathering. The western part of the Adiankoting area directly borders Central Tapanuli Regency and includes the Angkola volcanic formation, Barus formation, Klut formation, Martimbang volcanics, Sibolga complex, Toba tuff rocks, and Toru volcanics. Tracing the potential REE content aims to identify prospective areas by examining the megascopic and microscopic characteristics, as well as the distribution of rock types and their elemental composition, as reserves of natural resources in the Adian Koting area.

The results of tracing the potential REE-bearing rocks were determined using ore microscopy methods x-ray fluorescence (XRF) and inductively coupled plasma mass spectrometry (ICP-MS) (Vansla et al, 2023). The analysis of rare earth element-bearing content in rocks is carried out to determine the type and name of the rock, as well as the minerals contained in outcrop rocks. The ore microscopy method (polished section) is a geometallurgical approach that uses a polarizing microscope to examine the composition, texture, and structure of REE-bearing rocks (mineralogical associations of REE elements). Ore microscopy is an important method in mining exploration and development. The composition of REE elements is identified using the XRF method by utilizing the wavelength of individual material components from the fluorescence emission produced by the sample (Adeti et al, 2023). ICP-MS involves ionizing a sample in an inductively coupled plasma and then separating and quantifying the ions based on their mass-to-charge ratio using a mass spectrometer. ICP-MS is sensitive for analyzing REE at low concentrations (ppb–ppm).

REE concentration analysis using ICP-MS is capable of detecting small changes in element concentrations (Wysocka, 2021). The combination of petrological and geochemical methods provides complementary and comprehensive contributions for tracing the REE potential in Adian Koting area.

METHOD

Research location

Research samples were collected from the Adian Koting area in north Tapanuli, Indonesia (Figure 2). A total of 3 samples were randomly

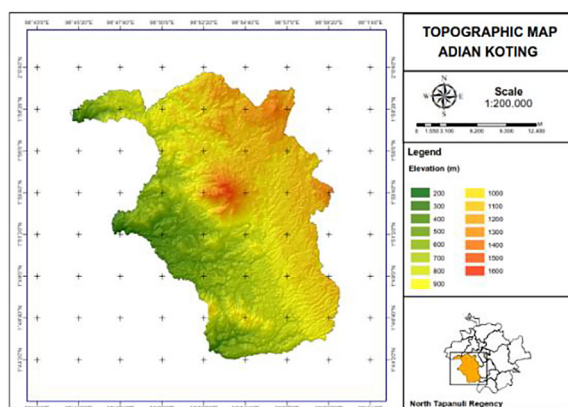


Figure 1. Topographic map Adian Koting area

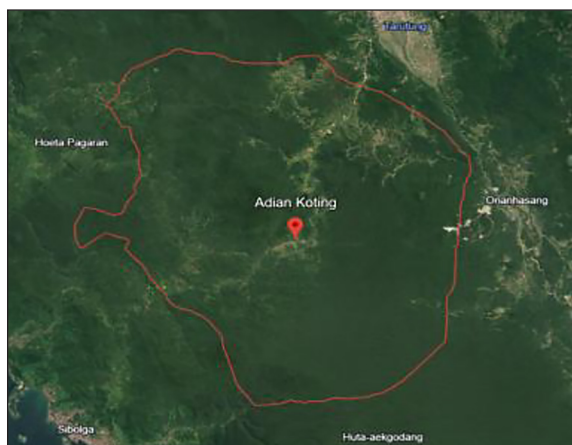


Figure 2. Research map location

collected using a Global Positioning System (GPS). The traced samples at the location were in the form of outcrop rocks (Figure 3).

MATERIAL AND METHODS

The rock samples were tested using petrological and geochemical methods, with petrological analysis conducted through polished sections and geochemical analysis using XRF and ICP-MS. Mineralogical analysis was carried out using the ore microscopy (mineragraphy) method to determine the composition, texture, type, and structure of the rocks. XRF testing was used to obtain the

elemental composition present in the samples, while ICP-MS was used to determine the element concentrations. The detailed research procedure is illustrated in the scheme shown in Figure 4.

A total of 3 samples were used for the ore microscopy method, randomly taken from outcrop rocks. The samples were prepared into polished sections following the steps shown in Figure 5.

The rock samples were cut into sizes of 2–3 cm with a thickness of 1–2 cm. The samples were mounted on glass slides using epoxy resin adhesive. The mounted glass slides were then thinned using a grinder. The thinning process reached approximately 30 microns (0.03 mm), followed by polishing with abrasive paper and cleaning and drying of the samples to remove any remaining abrasive material (Figure 6).

The samples were analyzed for mineral texture and structure using a Bestscope 5062TTR series polarizing microscope with 4x, 10x, and 40x objective lenses and a 10x eyepiece lens.

The results of ore microscopy are based on the megascopic characteristics of the rock and the microscopic features of the minerals.

Samples used for the XRF method aim to reveal or uncover the chemical fractionation processes within the geological system and provide distinct characteristics of the rock-forming minerals. A total of 3 samples were randomly collected from outcrop rocks. The samples were prepared



Figure 3. Outcrop rock samples

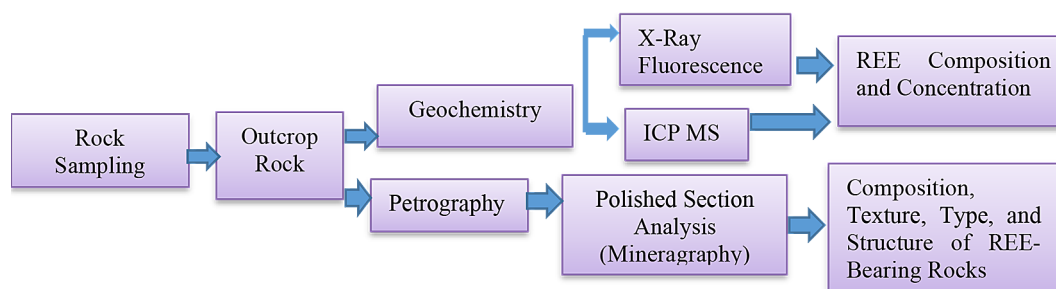


Figure 4. Research flowchart



Figure 5. Research procedures with ore microscopy method sample preparation



Figure 6. Ore microscopy sample

following the steps shown in Figure 7. Sample preparation was carried out to the procedure:

1. The samples were ground to a size of 200 mesh (Figure 8).
2. The samples were analyzed using XRF HD Mobile 1.2.6.IOP-M2 10WPS S7 4SS to determine the elemental composition of the rocks (Amira et al, 2021; Vansla et al, 2023; Juliani et al, 2024).
3. XRF results were analyzed for the content and composition of the samples.
1. Sample preparation involves grinding to a size of 200 mesh with a mass of 2 grams (Figure 10).
2. The sample is mixed with strong acids (such as HNO_3 , HF , or HCl) to dissolve the REE elements.
3. The instrument is calibrated using REE standards in the form of standard element solutions that include REEs such as La, Ce, Nd, Sm, Eu, Gd, Tb, Dy, Ho, Er, Tm, Yb, Lu, and Y.
4. The sample solution is introduced into the nebulizer system, which converts the liquid into a fine aerosol for ionization.
5. Data are read by the mass analyzer to obtain signal intensities for each element.
6. Detection and quantification are performed by observing the intensity received by the detector, which calculates and compares it with the calibration curve.
7. Signal intensity determines the concentration of REEs in the sample.

ICP-MS is a technique that combines inductively coupled plasma to break down the sample into ions, and mass spectrometry to identify and measure the elements in the sample. The rock sample is prepared following the steps shown in Figure 9. Procedure for using the ICP-MS method:



Figure 7. Research procedures using the ore microscopy method



Figure 8. XRF test sample preparation



Figure 9. Research procedures with metode ICP-MS



Figure 10. XRF sample preparation

RESULT AND DISCUSSION

The rock sample from the macroscopic examination is identified as a coherent igneous rock, specifically a plutonic rock in the form of granite. It has a light gray to white color with black specks, light brownish-white with reddish-brown to brown patches and black spots, and cream to grayish-white with black specks. The rock exhibits an equigranular (hypidiomorphic) texture, hypidiomorphic-granular; phaneritic (coarse-grained). The grain shape is predominantly subhedral, with a massive structure and a mineral composition of quartz, plagioclase, biotite, opaque minerals, and hornblende (Pettijohn et al., 2015).

The granite rocks in the Adian Koting area are intrusive (plutonic) igneous rocks formed from the solidification of acidic magma at depth within the Earth, spreading in a northwest-southeast direction. The granite is identified as part of a granitoid intrusion associated with the Sibolga complex. Granite serves as a host for the deposition and concentration of REEs. The group of granite units in the study area belongs to the ilmenite-series granite or S-type granite (Faisal and Nursahan, 2022).

The mineral content of the rock was analyzed using the ore microscopy method (polished section) by observing reflectance properties under a microscope with objective and ocular lenses.

The microscopic analysis revealed the presence of silicate minerals and ore minerals. Silicate minerals, composed of silicon (Si) and oxygen (O), are the primary constituents of the Earth's crust, known as rock forming materials (RFM), formed through the crystallization of magma into minerals that make up igneous rocks. The silicate minerals include quartz (qz), biotite (bt), chlorite (chl), hornblende (hbl), and rutile (rt). Silicate minerals are often found in association with ore deposit minerals, as detailed in Table 1.

The results based on Table 1 show the presence of chlorite (chl) minerals, indicating that the granite rock has undergone alteration (Indarto and Zulkarnain, 2008). Ore minerals contain one or more elements of economic value that can be extracted for industrial use. The ore minerals found in the rock samples include monazite (mnz), xenotime (xn), magnetite (mag), pyrochlore (phc), titanite (tn), pyrite (py), allanite (alt), zircon (zr), and arsenopyrite (asp). The content of ore-bearing minerals in the samples is summarized in Table 2.

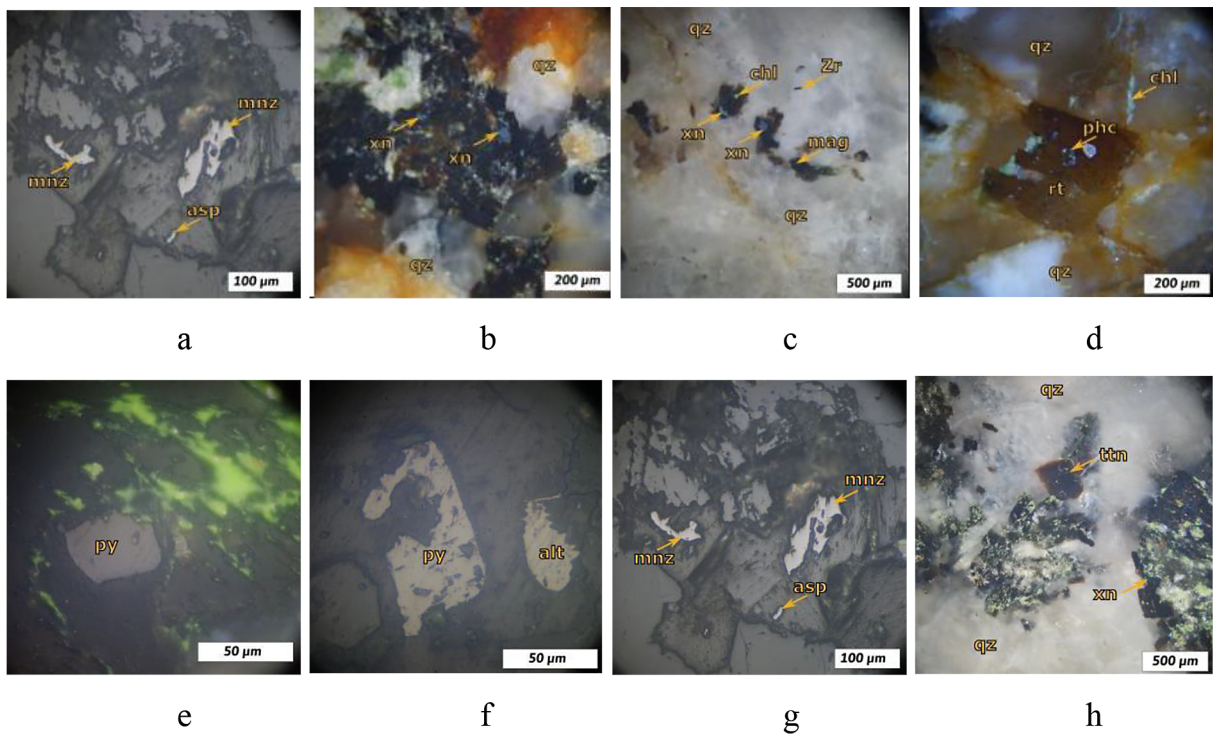
The ore minerals present in the rock samples are shown in Figures 11a–h. The ore minerals in Table 2 show the presence of REE-bearing minerals such as zircon, monazite, and xenotime. The presence of these REE-bearing minerals is due to the granite rock's content of silica (SiO₂), alumina (Al₂O₃), magnesium (Mg), and iron (Fe),

Table 1. Silicate mineral content

Silicate minerals	Mineral content					
	PG2		SAK		SB	
	Abundance (%)	Size (µm)	Abundance (%)	Size (µm)	Abundance (%)	Size (µm)
Quarsa (qz)	60	50–1284	50	100–1015	57	50–1020
Biotite (bt)	*	-	20	9–30	15	50–500
Clorite (chl)	10	10–50	-	-	4	20–50
Hornblende (hbl)	-	-	-	-	7	20–150
Rutile (rt)	-	-	-	-	<1	50

Table 2. Ore mineral content of the rock

Ore Mineral	Mineral content					
	PG2		SAK		SB	
	Abundance (%)	Size (μm)	Abundance (%)	Size (μm)	Abundance (%)	Size (μm)
Monazite (mnz)	1	7-30	1	10-50	1	10-30
Xenotime (xn)	3	20-50	1	9-30	1	30
Magnetite (mag)	1	20	2	30-70	-	
Pyrochlore (phc)	-	-	< 0.1	25	< 0.1	6-15
Titanite (tn)	1	20	-	-	-	
Pyrite (py)	2	20-40	1	30	-	
Allanite (alt)	<0.1	15	-		-	
Zircon (zr)	<0.1	20	-		-	
Arsenopyrite (apy)	<0.1	30	-		-	

**Figure 11.** Ore minerals in the rock sample

which are associated with gangue minerals and REE minerals. Zircon (zn) has a high refractive index and strong color dispersion. Zircon specimens can appear yellow, gray, green, brown, blue, or red (Figure 11b). Brown zircon, when heat-treated, can change to blue. Zircon minerals form prismatic to dipyrarnidal crystals. Zircon is commonly found in metamorphic rocks and silica-rich igneous rocks (Bonewitz, 2012). Zircon is a zirconium silicate mineral that contains thorium, yttrium, and cerium (Suprpto, 2016). Xenotime (xn) is a phosphate mineral containing

yttrium and other rare earth elements. Xenotime appears as dark bluish-gray inclusions within biotite or quartz (Figure 11c). Monazite and xenotime are often found in tin and gold deposits. Xenotime contributes as a carrier of REE Y and is classified as a HREE (heavy rare earth element). Monazite (mnz) is found in granite rock samples as alluvial deposits resulting from water activity. Monazite contributes as a carrier of REEs such as Ce, La, Nd, Th, and Sm. The phosphate mineral monazite-(Ce), or cerium phosphate, appears yellowish to reddish-brown, brown,

greenish, or nearly white. Monazite-(Ce) crystals are prismatic, tabular, or elongated, sometimes large and coarse, and often twinned (Figure 11g). Two other monazite species are monazite-(La), or lanthanum phosphate, and monazite-(Nd), or neodymium phosphate. The Adian Koting area shows a contact zone between the intrusion and the surrounding rocks, with hydrothermal alteration indicated by the presence of chlorite, magnetite, pyrite, and quartz veins. Chlorite is an alteration product of biotite, formed through mineral transformation during alteration. The deposition of minerals in the granite rock is associated with a hydrothermal system that occurred during magmatic activity. Minerals undergo alteration through the circulation of hydrothermal fluids along fracture structures and minor faults. Hydrothermal alteration in granite involves the chemical replacement of original minerals by new ones due to interaction with hydrothermal fluids. This interaction process can result in various alteration minerals, including chlorite, sericite, clay minerals, and secondary quartz. The specific minerals formed depend on factors such as temperature, fluid composition, and the rock's microstructure. The granite intrudes into low- to medium-grade metamorphic rocks.

Rare earth element content

The content of REE elements in the Adiankoting area was analyzed using XRF, revealing the presence of Ce and La elements. The concentration of Ce ranged from 74.3 to 97.5 ppm, with the highest value found at the SAK location (97.5 ppm) and the lowest at SB (74.3 ppm). The La content ranged from 90.2 to 141.0 ppm, with the highest at SAK and the lowest at SB (90.2 ppm). The detailed distribution of REEs is shown in Table 3. The abundance of REE elements tends to increase (enrichment) or decrease (depletion) due to weathering, which leads to mobilization and fractionation. The La content is transported from its primary carrier minerals and reabsorbed into minerals undergoing weathering (Sanematsu and Watanabe, 2016).

The presence of Ce and La elements in the Adian Koting area is the result of the weathering and breakdown of rocks from the Sibolga complex in association with granite rocks (Juliani et al., 2024). The intrusion of the Sibolga complex into the Kluet Formation caused low-grade metamorphism below the amphibolite facies, forming quartzite, schist and pelitic gneiss, mylonite and cataclastic rocks, as well as hornfels (Hidayati et al., 2022). The rare earth element (REE) content that is adsorbed originates from the decomposition of groundwater interacting with granite rocks. Oxidized rare earth elements are transported and deposited from the upper layers. The enrichment of light rare earth elements (LREE) is higher than that of heavy rare earth elements (HREE).

The REE-bearing rocks formed in the Adian Koting area are part of a back-arc magmatic belt dating from the Cretaceous to Eocene, which formed granitic rocks. The magmatic process began with partial melting of the continental crust, producing granite with garnet fractionation (negative anomaly in heavy REEs) at a depth of 70 km, followed by plagioclase Ca fractionation (negative Eu and Sr anomalies) at shallower depths (SDM, 2019).

The presence of REE elements based on ICP-MS results in Table 4 indicates the potential of REE-bearing minerals such as Sc, La, Ce, Pr, Nd, Sm, Gd, Dy, Tb, Er, Tm, Yb, Lu, Eu, and Ho. The elements Ce, La, Nd, Th, and Sm are contributed by the monazite minerals found in the granite igneous rock samples. The element Y, classified as a heavy rare earth element (HREE), is present in xenotime with a concentration of 4.211 ppm in the sample. Zircon, a zirconium silicate mineral, contains thorium, yttrium, and cerium. ICP-MS test results show the presence of REEs with dominant concentrations of Sc (3.5–5.5%), La (4.1–5.6%), Y (4–6.1%), Ce (3.5–4.8%), Gd (3.9–5.8%), Tm (5.4–5.6%), and Eu (3.1–5.1%). The REEs with minimum concentrations include Dy (1.9–3.6%), Yb (0.8–3.5%), and Er (0.473–84.4%).

REEs are present in granite rocks, which are formed from silica-rich magma. Acidic magma tends to contain more REE elements compared to mafic or intermediate magma. The crystallization

Table 3. REE content in the Adiankoting area

No	Element		Concentration (ppm)								
			PG2			SAK			SB		
1	Ce	Cerium	86.0	81.5	83.2	86.0	90.6	96.6	97.5	75.1	74.3
2	La	Lanthanum	135.0	125.0	130.0	135.0	132.0	137.0	141.0	103.0	104.0

Table 4. REE Content in the Adiankoting area

Sample	Concentration (ppm)															
	Sc	La	Y	Ce	Pr	Nd	Sm	Gd	Dy	Tb	Er	Tm	Yb	Lu	Eu	Ho
SAK	1.271	16.280	4.211	16.256	3.919	13.556	2.646	3.560	1.599	0.376	84.4	84.0	1.031	0.088	0.446	0.305
Concentration (%)	5.5	5.6	6.1	3.5	4.3	3.6	4.4	5.8	3.6	5.1	1.6	5.4	3.5	1.9	3.5	4.7
PG2	0.729	7.215	2.169	16.873	1.539	5.821	0.999	2.279	0.771	0.192	0.450	0.067	0.473	0.039	0.98	0.152
Concentration (%)	3.5	4.1	4.0	4.8	3.6	4.5	3.1	3.9	1.9	2.7	3.0	5.6	0.8	6.1	5.1	3.5

process of acidic magma within the Earth's crust can separate REE elements into minerals that are more resistant to weathering. The intensity of REE presence is shown in Figure 12, and the REE content levels are displayed in Figure 13.

The REE concentrations shown in Figures 12 and 13 indicate the presence of all REE elements. REEs are commonly categorized into two subgroups: LREE and HREE. Elements from 57La to 63Eu are considered LREEs, while elements from 64Gd to 71Lu, including Y, are categorized as HREEs. Both REE categories are typically found in the same deposits, except for Sc. Therefore, Sc is not included in the above subgroups. In general, LREEs are more abundant than HREEs.

The lithology of REE-bearing rocks at the sampling points produced a geological map at a scale of 1:220,000. The dominant rock samples originate from the Kluet Formation (%) marked in light blue, and the Sibolga Complex (%)

marked in green, which are Paleozoic-aged rocks (Hidayati et al., 2022). The Kluet Formation is intruded by the Sibolga Complex, which underwent low-grade metamorphism below amphibolite facies, forming quartzite, schist and pelitic gneiss, mylonite and cataclastic rocks, as well as hornfels (Faisal et al., 2022).

The Sibolga Complex at the sampling locations consists of granite rocks. The lithic tuff unit, gray in color (%), generally composes the eastern part of the Adian Koting area. These rock types—granodiorite, granite, and diorite—are believed to have formed in the Early Permian due to the subduction of the Paleo-Tethys (Figure 14). Based on the geological map of the Adian Koting area, the estimated amount of REE contained in the Sibolga Complex is 173,546,672,283 m³ (Table 5).

This potential is primarily associated with the intrusion of granitoid rocks and hydrothermal alteration zones that have affected both these rocks

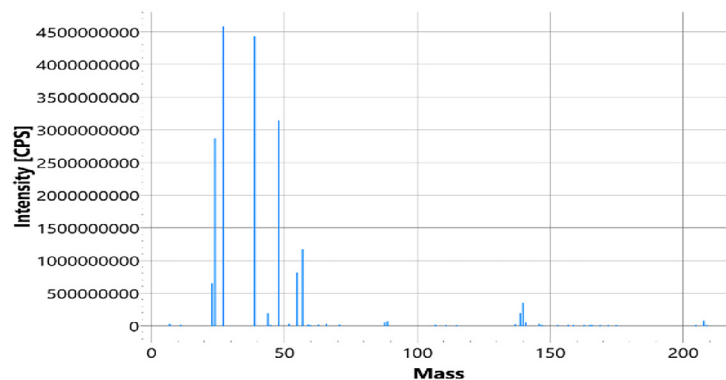
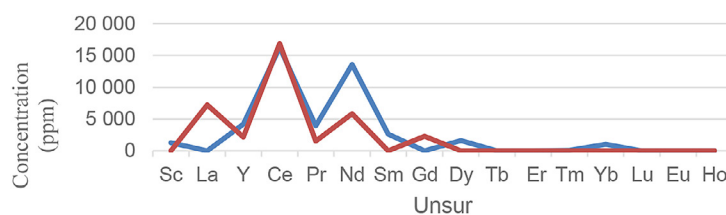
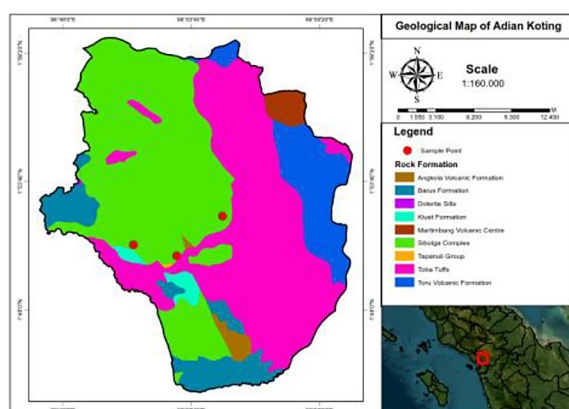
**Figure 12.** Intensitas element REE**Figure 13.** Concentration graph REE

Table 5. Area and volume of formations in the Adian Koting Area

Formation	Shape area (m ²)	Mean elevation (m)	Volume (m ³)
Angkola volcanic formation	5814900,06	800	4.651.920.048
Barus formation	37404309,15	600	22.442.585.490
Dolerite sills	184381,33	600	110.628.798
Kluet formation	6684015,94	600	4.010.409.564
Martimbang volcanic centre	8201295,93	1400	11.481.814.302
Sibolga complex	192829635,87	900	173.546.672.283
Tapanuli group	210173,76	700	147.121.632
Toba tuffs	180551089,91	800	144.440.871.928
Toru volcanic formation	46622604,18	1100	51.284.864.598

**Figure 14.** Lithology map of Adiankoting

and the surrounding metamorphic rocks. Petrographic analysis shows the presence of accessory REE-bearing minerals, and ICP-MS geochemical analysis confirms anomalies in REE concentrations, particularly LREEs. These findings support the hypothesis that Adian Koting is a prospective area for REE exploration.

CONCLUSIONS

Results obtained from polished thin section analysis show that the rock is a coherent, plutonic igneous rock, specifically granite, with a light gray to white color and black specks, brownish-white with brick-red to brown patches and black spots, and cream to grayish-white with black specks. The rock has an equigranular, hypidioritic-granular, and phaneritic texture. It has a predominantly subhedral grain shape and a massive structure, composed of quartz, plagioclase, biotite, opaque minerals, and hornblende. Microscopically, REE-bearing minerals such as zircon, monazite, and xenotime were identified.

Monazite appears in prismatic, tabular, or elongated crystal forms, sometimes large, coarse, and commonly twinned. Monazite and xenotime are found in association, with their presence as inclusions in biotite or quartz indicating early crystallization. Zircon appears as small, bright-colored inclusions. REE content in the Adian Koting area, based on XRF analysis, shows the presence of Ce and La elements, with Ce concentrations ranging from 74.3 to 97.5 ppm and La from 90.2 to 141.0 ppm. ICP-MS results show the presence of REEs with dominant concentrations of Sc (3.5–5.5%), La (4.1–5.6%), Y (4–6.1%), Ce (3.5–4.8%), Gd (3.9–5.8%), Tm (5.4–5.6%), and Eu (3.1–5.1%). The REEs with lower concentrations include Dy (1.9–3.6%), Yb (0.8–3.5%), and Er (0.473–84.4%). The presence of REEs indicates that the Adian Koting area holds significant potential as a natural resource for high-tech industrial materials.

Acknowledgment

The authors would like to thank Medan State University for facilitating and funding this research. The team also thanks the KDBK Earth Physics for its support and encouragement throughout this research. The research was funded under the “Penelitian Produk Terapan” scheme with contract number: 0055/UN33.8/PPKM/PPT/2025, therefore the author would like to thank the Rector Universitas Negeri Medan.

REFERENCES

- Adeti P.J., Amoako G., Tandoh J.B., Gyampo O., Ahiamadjie H., Amable A.S.K., Kansaana C., Annan R. A.T., B. A. (2023). Rare-earth element comparative analysis in chosen geological samples using

- nuclear-related analytical techniques, Nuclear Instruments and Methods in Physics. *Research Section B: Beam Interactions with Materials and Atoms*, 2(1), 122–128. <https://www.sciencedirect.com/science/article/abs/pii/S0168583X23001301>
2. Adam H. (2016). Logam Tanah Jarang: Cadangan Strategis Masa Depan Indonesia. [https://www.kompasiana.com/harristioadam/58289544137b61950616caff/logam-tanah-iarang-cadangan-strategis-masa-depan%20indonesia%20page=all?page=all&page_images=2%202024\)#goog_rewarded](https://www.kompasiana.com/harristioadam/58289544137b61950616caff/logam-tanah-iarang-cadangan-strategis-masa-depan%20indonesia%20page=all?page=all&page_images=2%202024)#goog_rewarded)
 3. Bonewitz R. L. (2012). *Nature Guide Rocks and Minerals. Published in the United States by DK Publishing 375 Hudson Street.* <https://archive.org/details/nature-guide-rocks-and-minerals-dk-2012>
 4. Castor, S. B., Hedrick, J. B. (2006). Rare Earth Elements. In *Industrial Minerals & Rocks: Commodities, Markets, and Uses. Society for Mining, Metallurgy, and Exploration.*, 7(1), 769–792. <https://www.scirp.org/reference/referencespapers?referenceid=2142069>
 5. Dushyantha N., Batapola N., Ilankoon I.M.S.K. I, Rohitha S., Premasiri R., Abeyasinghe B., Ratnayake N, D. K. (n.d.). The story of rare earth elements (REEs): Occurrences, global distribution, genesis, geology, mineralogy and global production Ore. In *Geolog Reviews Elsevier* 122. (July 2020, 103521). <https://www.sciencedirect.com/science/article/abs/pii/S0169136820300937>
 6. Faisal R.M, Nursahan I, N. R. S. (2022). Penyelidikan umum logam tanah jarang dengan metoda pengeboran di daerah parmonangan kabupaten tapanuli utara provinsi sumatera utara, prosiding hasil kegiatan anggaran 2022. *Pusat Sumber Daya Mineral Batubara Dan Panas Bumi Tahun*, https://geologi.esdm.go.id/perpustakaan?p=show_detail&id=24
 7. Firman F., Haya A., Sahidi A.Z., (2020). Identifikasi kandungan logam tanah jarang pada abu batubara PLTU mulut tambang, *Jurnal Geomining* 1(1), April 2020 (18–24). <https://ejournal.unkhair.ac.id/index.php/geomining/article/view/2089>
 8. Hasnur R., Setijadji L.D, Warmada I.W, (2010). Potensi pembentukan endapan laterit unsur tanah jarang (Ree) di Indonesia, *Proceedings Pit Iagi Lombok 2010* The 39th IAGI Annual Convention and Exhibition. https://www.iagi.or.id/web/digital/12/2010_IAGI_Lombok_Potensi-Pembentukan-Endapan.pdf
 9. Hidayati A.Nurul, Basuki N I, Sulaeman, S. B. (n.d.). Distribution of major elements and rare earth elements in the weathered granitoid rocks in the Parmonangan area, North Tapanuli Regency. *Buletin Sumber Daya Geologi*, 17(3), 149–162. https://buletinsdg.geologi.esdm.go.id/index.php/bsdg/article/view/BSDG_VOL_17_NO_3_2022_2/314
 10. Idris, M. (2023). Mengenal logam tanah jarang atau rare earth yang bikin geger se-Eropa,. *Kompas.Com*, 2. <https://money.kompas.com/read/2023/01/14/112117826/mengenal-logam-tanah-jarang-atau-rare-earth-yang-bikin-geger-se-eropa?page=all>
 11. Indarto S, Zulkarnain I, S. I. D. S. (2008). *Mineralisasi Pada Batuan Plutonik Dan Volkanik Daerah Kotanopan Dan Panyabungan, Mandailing Natal, Sumatera Utara., Prosiding Pertemuan Ilmiah Tahunan IAGI KE-37.* https://www.iagi.or.id/web/digital/14/2008_IAGI_Bandung_Mineralisasi-Pada-Batuan.pdf
 12. Juliani R, Rahmatsyah, Tambubolon T, Halawa E, Sari S.D, (2024). Characteristics of Rare Earth Metals Rock Content in the Parmonangan Area of North Tapanuli Using Petrographic Methods. *Journal of Physics: Conference Series* 2908 (2024) 012026. <https://iopscience.iop.org/article/10.1088/1742-6596/2908/1/012026/meta>
 13. Kementerian Energi dan Sumber Daya Mineral. (2019). *Potensi Logam Tanah Jarang di Indonesia*. Bandung: Pusat Sumber Daya Mineral, Batubara dan Panas Bumi. https://geologi.esdm.go.id/perpustakaan/?p=show_detail&id=1306&keywords=
 14. Middelburg, J.J., van der Weijen, C.H, Woittiez, J.R. (1988). Chemical processes affecting the mobility of major, minor and trace elements during weathering of granitic rocks. *Chemical geology*, 68(3–4), 253–273 https://www.researchgate.net/publication/223346358_Chemical_processes_affecting_the_mobility_of_major_minor_and_trace_elements_during_weathering_of_granitic_rocks
 15. Nesse, W.D., (2013). *Introduction to Optical Mineralogy 4th Ed.* Oxford University Press, Oxford, 361. <https://www.geokniga.org/bookfiles/geokniga-introductiontoopticalmineralogy.pdf>
 16. Ngadenin, Karunianto A. J, Indrastomo F. D, (2020). Penentuan daerah prospek logamtanah jarang di pulau singkep determination of rare earth elements prospect Area in Singkep Island. *Eksplorium*, 41(1), Mei 2020: 15–24. <https://ejournal.brin.go.id/eksplorium/article/view/8035>
 17. Pettijohn, F.J., Potter, P.E., and Siever, R. (2015). *Sand and Sandstone. 2nd Edition, Springer-Verlag, New York.* <https://www5.unin.it/Biblioteca/it/Web/EngibankFile/Sand%20and%20sandstone.pdf>
 18. Puspita M, Arsyad A.R, Wahyudi Zahar, (2022), Identification of rare earth metal elements in the coal coal at pt. prima mulia sarana sejahtera, Muara Enim Regency, South Sumatra Province. *Comserva*, 1(9), 657–666. https://www.researchgate.net/publication/360625836_Identifikasi_Keterdapatan_Unsur_Logam_Tanah_Jarang_dalam_Lapisan_Batubara_di_PT_Prima_Mulia_Sarana

- Sejahtera_Kabupaten_Muara_Enim_Provinsi_Sumatera_Selatan/fulltext/637f8133554def619368a3eb/Identifikasi-Keterdapatan-Unsur-Logam-Tanah-Jarang-dalam-Lapisan-Batubara-di-PT-Prima-Mulia-Sarana-Sejahtera-Kabupaten-Muara-Enim-Provinsi-Sumatera-Selatan.pdf
19. Rasyid, R. (2011). Perbandingan x-ray fluorescence (XRF) dan inductively coupled plasma-optical emission spectrophotometer (ICPOES) untuk analisis nikel dan besi dalam sampel converter slag pada industri pertambangan nikel. <https://dspace.uui.ac.id/handle/123456789/33603>
 20. Ritonga, R., (2022). *Studi Keterdapatan dan Pengayaan Logam Tanah Jarang (LTJ) pada Batuan Vulkanik Formasi Adang Kabupaten Mamuju Provinsi Sulawesi Barat*. Thesis, Universitas Hasanuddin. <https://repository.unhas.ac.id/id/eprint/12245/>
 21. Ravisankar R., Manikandan E., Dheenathayalu M., Rao B, Seshadreesan N.P, Nair K.G.M., (2006), Determination and distribution of rare earth elements in beach rock samples using instrumental neutron activation analysis (INAA), *Nuclear Instruments and Methods in Physics Research Section B: Beam Interactions with Materials and Atoms* 251(2), October 2006, 496–500.
 22. Sanematsu, K., Watanabe, Y. (2016). Characteristics and genesis of ion adsorption type deposits. *Rev. Econ. Geol.*, 18(2), 55–79. <https://pubs.geoscienceworld.org/segweb/books/edited-volume/1998/chapter-abstract/16271168/Characteristics-and-Genesis-of-Ion-Adsorption-Type?redirectedFrom=fulltext>
 23. Suprpto, S. J. (2009). Tinjauan tentang Unsur Tanah Jarang. *Buletin Sumber Daya Geologi*, 4(1), 36–47. https://buletinsdg.geologi.esdm.go.id/index.php/bsdg/article/view/BSDG_VOL_4_NO_1_2009_4#:~:text=Abstract,daya%20yang%20potensi%20untuk%20dusahakan
 24. Vansla, T., Rahman, H.A., HAR, Rusli., F. (2023). Kajian potensi logam tanah jarang pada batupasir formasi ombilin atas dan formasi ombilin bawah menggunakan analisis x-ray fluorescence. *Jurnal Bina Tambang*, 8(2), 146–153. <https://paperity.org/p/338089924/kajian-potensi-logam-tanah-jarang-pada-batupasir-formasi-ombilin-atas-dan-formasi-ombilin>
 25. Wysocka I. (2021). Determination of rare earth elements concentrations in natural waters – A review of ICP-MS measurement approaches. *Talanta Elsevier*, 2(1). <https://www.sciencedirect.com/science/article/abs/pii/S0039914020309279>